**Atmospheric
Measurement
Techniques**

Water vapor total column measurements using the Elodie Archive at Observatoire de Haute Provence from 1994 to 2004

A. Sarkissian[1] and J. Slusser[2,*]

[1]LATMOS, CNRS UMR 8190, Université Versailles Saint-Quentin, Université Pierre et Marie Curie, Institut Pierre-Simon Laplace, 91371 Verrières-le-Buisson, France
[2]USDA, UV-B Radiation Monitoring Program, NREL, Colorado State University, Fort Collins, CO 80521, USA
[*]now retired

Abstract. Water vapor total column measurements at Observatoire de Haute Provence (5°42′ E, +43°55′ N), south of France, were obtained using observations of astronomical objects made between July 1994 and December 2004 on the 193-cm telescope with the high-resolution spectrometer Elodie. Spectra of stars, nebulae, and other astronomical objects were taken regularly during 10 years. More than 18 000 spectra from 400 nm to 680 nm are available on-line in the Elodie Archive. This archive, usually explored by astronomers, contains information to study the atmosphere of the Earth. Water vapor absorption lines appear in the visible in delimited bands that astronomers often avoid for their spectral analysis. We used the Elodie Archive with two objectives: firstly, to retrieve seasonal variability and long-term trend of atmospheric water vapor, and secondly, to remove signatures in spectra for further astronomical or geophysical use. The tools presented here (the workflow, the interoperable Elodie Archive and the web service Tellodie) are developed following, when possible, formats and standards recommended by the International Virtual Observatory Alliance.

1 Introduction

The Elodie archive is a database of high-resolution spectra of astronomical objects (spectral domain: 385 nm to 680 nm; sampling 0.005 nm; resolution: 0.0065 nm) obtained with the Elodie spectrograph on a 193-cm diameter telescope at Observatoire de Haute Provence (5°42′ E, +43°55′ N, altitude

681 m) from July 1994 to December 2004 (Moultaka et al., 2004). Note that Sophie spectrograph replaced the Elodie Spectrograph in July 2005 but the Sophie archive was not open when we started this work. More than 18 000 spectra of stars, galaxies, and other astrophysical objects are available in the Elodie archive (the ELODIE archive presently contains 34 992 spectra, among which 18 318 were public when we started this work), accessible using an online web service or php protocol. This database is updated regularly, when spectra with restricted access are opened to the community, or after updating the pipeline of the processing. The archive allows wider use of existing data sets, and this paper applies Virtual Observatory (VO) concepts of the workflow (Appendix A), see the International Virtual Observatory Alliance (IVOA, 2007) web site at http://www.ivoa.net/ and references therein for details. Initially developed for presentation to students using the "hot" theme of exoplanet search (Sarkissian, 2007), this tool is used here in geophysical application of the atmospheric water vapor budget.

The composition of the Earth's atmosphere is of great interest not only to atmospheric scientists but also to astronomers for whom the atmosphere is an annoyance to be removed in order to interpret astronomical observations without interference from terrestrial gases and aerosol. Intensive astronomical stellar spectroscopic observations began in the early 20th century. Fowle (1912) pioneered the determination of atmospheric water vapor from infrared absorption lines in the solar spectrum. Challonge and Divan (1952) pioneered the determination of atmospheric ozone from UV astronomical stellar spectral observations. We present a study of terrestrial atmospheric water vapor derived from astrophysical observations in the visible. Water vapor in the atmosphere has become increasingly important due to its strong feedback to global warming by man-made greenhouse gas

emission. The involvement of water vapor in the stratospheric ozone equilibrium is related to tropospheric water vapor convection and troposphere-stratosphere exchanges. Water vapor in the atmosphere plays a crucial role since water vapor absorbs the longwave radiation of the Earth's surface. The amount of water vapor is expected to increase with temperature (Clausius-Clapeyron equation) so that a water vapor feedback can amplify global warming by anthropogenous greenhouse gas emissions. Long-term monitoring of atmospheric water vapor is mandatory for a better understanding and prediction of climate change (Held and Soden, 2000).

The current paper makes available water vapor column measurements from both recent and long term astrophysical observations. Common techniques to retrieve water vapor on site for astrophysical observations have always been without telescope dependent instruments, for instance: surface humidity sensors or precipitable water vapor sensor. Spectrometric observational methods are difficult, however, because line or band intensity and broadening depend on ambient temperature and pressure, requiring vertical profile rather than altitude on the line of sight, see Angione (1987), and references therein. We believe that this difficulty is now partly solved by improvement of spectral analysis techniques.

Measurements of water vapor by UV-visible spectrometers from the ground on direct sun, zenith sky, or from space on nadir sky has been demonstrated by Wagner et al. (2003). The most common method to measure atmospheric absorbants by UV-visible spectrometry is the Differential Optical Analysis Spectroscopy (DOAS), (Perner and Platt, 1979; Vaughan et al., 1997; Fayt and Van Roozendael, 2001; Sarkissian, 1992, 2000). Using Global Positioning System (GPS) and its signal time delay due to the atmosphere, one can make use of the satellite network of detectors and readily available handheld units to measure column water vapor (Bastin et al., 2005; Champolion et al., 2004). Infrared atmospheric sensors (Schneider et al., 2006), lidar (Hoareau et al., 2009), passive microwave radiometry (Westwater et al., 2005) and radio techniques also provide measurements of water vapor, vertical profiles or total amount. The existing network of these instruments, developed at the end of the last century for long term studies, will probably not grow to include more sites. The water vapor measurement presented here would continue to be available on-line at Tellodie web service (http://bdap.ipsl.fr/tellodie/, 2009) with regular updates (the Elodie full Archive, the Sophie Archive, etc.) to the scientific community.

The following section presents an overview of the spectral analysis. Section 3 presents the spectrum of the water vapor absorption cross-section. Section 4 describes in more details the spectral analysis, and Sect. 5 presents the results on 18 318 spectra. Description of a workflow in the VO is given in Appendix A.

2 Spectral analysis: overview

The spectral analysis has been specially developed for water vapor removal for future astrophysical use of the spectra. The authors' initial objective was to develop a spectral analysis to search water vapor signatures in external sources like exoplanets and bodies of the solar system. First analysis shows that water vapor signature in the visible in exoplanets is so tiny (optical thickness of 10^{-9} at most) that its detection is not possible with existing techniques, but in the infrared, water vapor, ozone and carbon dioxide absorption can reach a significant percentage, justifying development of this technique.

In atmospheric research, most spectrometric instruments use solar light as the source. The differential optical absorption spectroscopy (DOAS) method is used commonly for tiny absorptions because scattered light from zenith sky at twilight has path lengths up to 20 air masses (Sarkissian et al., 1995). Here, because the source is not always the same, the DOAS method cannot be applied and an absolute method had to be developed for Elodie. An example of a spectrum of the Elodie archive is presented in Fig. 2. The spectral range around 592 nm is displayed in Fig. 3. Not all astronomical spectra have as many visible absorption lines that are proper to solar type stars, here 51 Peg of spectral type G2. Some astronomical objects have only broad or a few lines visible, like hot O stars, or sometimes emission lines like nebulas. The wide range of sources make the spectral analysis more difficult, as we will discuss in the Sect. 5. If I_0 is the spectrum of the astronomical object outside the atmosphere, and taking into account the absorption by water vapor only, the Beer-Lambert law gives

$$I_{\text{observed}} = I_0 \times e^{-\tau_{\text{H}_2\text{O}}}, \tag{1}$$

where I_{observed} is the intensity of the observed spectrum and $\tau_{\text{H}_2\text{O}}$ the water vapor optical thickness in the observed spectrum. We called here our analysis an absolute method compared to the DOAS one because we compensate water vapor signature in the observed spectra adding a negative absorption (i.e. equivalent to an emission) at intensity levels instead of doing it at differential intensity level,

$$I_{0,\text{calculated}} = I_{\text{Elodie}} \times e^{+\tau_{\text{H}_2\text{O}}}, \tag{2}$$

where I_{Elodie} is the intensity (in counts) of the spectrum observed by the Elodie spectrometer, $I_{0,\text{calculated}}$ the spectrum calculated without water vapor signature and $+\tau_{\text{H}_2\text{O}}$, the measured water vapor optical thickness in the observed spectrum. Absolute methods are often used when signal-to-noise ratio of observation is so low that differentiation will generate too much noise for use. Because of the very high quality of spectra needed in astronomy, most spectra (up to 96.5%) were used in the analysis. Then, the amount of water vapor molecules in the line-of-sight of the observation, $n_{\text{H}_2\text{O}}$, is

obtained by

$$\tau_{H_2O} = \sigma_{H_2O} \times n_{H_2O}, \tag{3}$$

where σ_{H_2O} is the water vapor absorption cross-section, derivable by means of a line list (Fally et al., 2003) under consideration of instrumental and observational characteristics, as presented below.

3 Water vapor absorption cross-section

Building the spectrum of the water vapor absorption cross-section from the line list was made in two steps: first, building a very high resolution and over-sampled set of cross-sections that can be adapted, as a second step, to each Elodie spectra when making spectral analysis. The high resolution cross-section is then kept as an input for the spectral analysis. This approach is time consuming, but guarantees the accuracy of the final resolution reached. In our case, a water vapor absorption cross-section is calculated from the on-line list at http://www.ulb.ac.be/cpm (2007), of water vapor line parameters, from 26 000 to 13 000 cm^{-1} (respectively, 770 nm to 385 nm) measured at 291.3 K (Coheur et al., 2002; Fally et al., 2003), with a portable high-resolution (0.06 cm^{-1}) Fourier Transform spectrometer within a 602-m long absorption cell. Table 1 summarizes modifications applied to the original list to build water vapor cross-section for Elodie spectra. Water vapor lines have a Voigt profile dominated by self-broadening and air-broadening modulated by air temperature and pressure variability on the line-of-sight of the telescope. We used a Gaussian weighting function when building the water vapor cross-section, because during analysis, an empirical Gaussian fit had a lower residual compared to other simple convolutions (see Sect. 5 for explanation on residuals). We also noted that vertical retrieval of atmospheric pressure and temperature seems to be possible using the water vapor line shape at these wavelengths, something to be explored in the future (Liu et al., 2006). Also, wavelength shift is calculated during spectral analysis, and no corrections were made compared to vacuum values when building the cross-section. Fig. 1 shows atmospheric water vapor lines convoluted with a Gaussian of 0.2 cm^{-1} width sampled at 0.01 cm^{-1}. Markers indicate the spectral position and the intensity in the original list. This set, converted into wavelength scale, was used as the starting point for the analysis of all spectra. This high resolution cross-section is convoluted by a Gaussian of R_{H_2O} nm Half Width Half Maximum (HWHM), resampled at Elodie spectral sampling, i.e., at 0.005 nm (0.13 cm^{-1} at 590 nm) for each spectrum individually. R_{H_2O} varies during the spectral analysis in order to cover all possible resolutions for Elodie spectra, i.e., from approximatively 0.08 to 0.12 nm, see Table 2.

The wavelength range chosen for the analysis is 591.5 to 593 nm because it includes two water vapor triplets (see Figs. 3 and 4) and is easy to identify visually as well as through dedicated software. The choice of a narrow (few
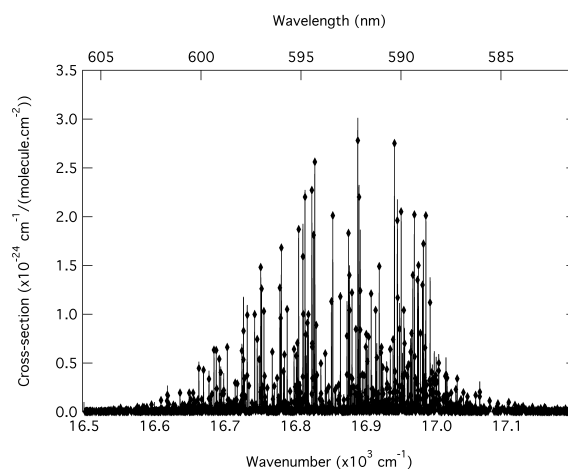

Fig. 1. H$_2$O absorption cross-section between 585 and 605 nm. The line list presented as markers is provided by Coheur et al. (2002) and Fally et al. (2003). The cross-section is calculated by convolution of the line list using a 0.17 cm^{-1} (0.0065 nm) HFWM Gaussian.
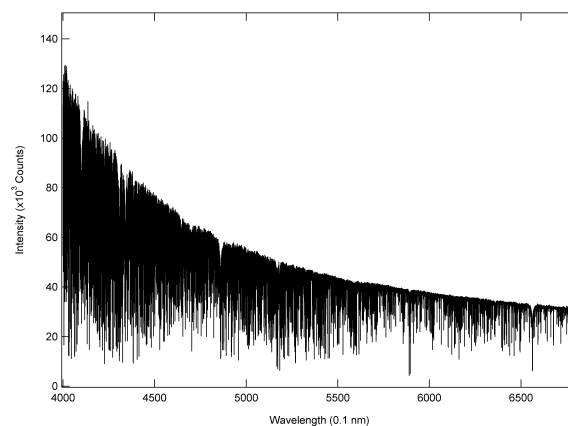

Fig. 2. Example of Elodie spectra: 51 Peg of spectral type G2 taken by Mayor and Queloz on 6 November 1995.
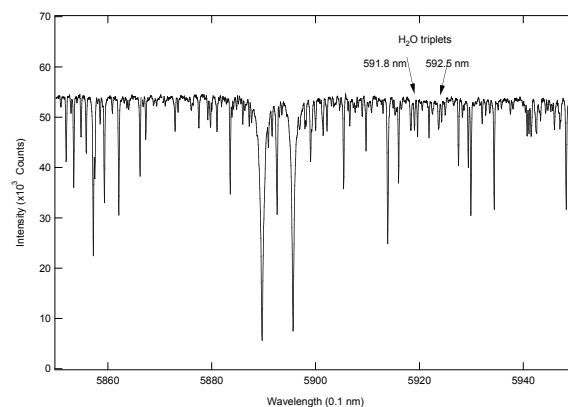

Fig. 3. Example of Elodie spectra (see Fig. 2), but focused on the water vapor absorption region at around 590 nm. Note the triplet at 591.8 nm, followed by the triplet at 592.5 nm.
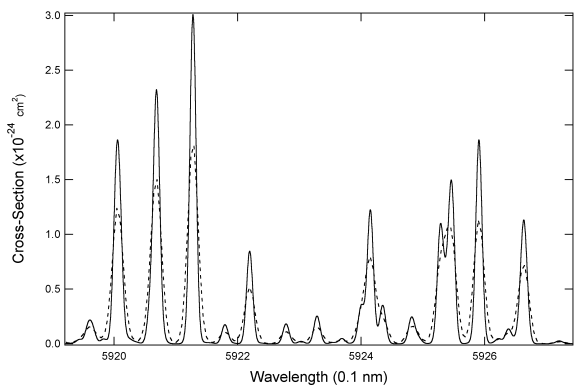
Fig. 4. H_2O cross-section (dotted line) resampled to Elodie HWHM (calculated from spectrum 199511060011 of 51 Peg) from initial cross-section (full line). Broadening and shift are calculated by minimizing the residual after substraction (see text).

nanometers wide) wavelength spectral range is due to the low probability of interference with similar intensity stellar spectral lines, as indicated by several runs made during analysis improvements. Also, the compromise between fast spectral analysis and the accuracy needed justifies such a narrow spectral range.

Saturation problems are common with strong water vapor absorption lines in the visible, and are usually corrected by a coefficient applied on the final result: a modified Langley technique (Michalsky et al., 1995; Wagner et al., 2003). Because the lines at 592 nm are so weak, our water vapor cross section are not corrected, and therefore do not take into account this effect. Discussion on this non-linearity of water vapor cross-section is in Sect. 6.

4   Observations

Observation of astronomical objects with Elodie, on the 193-cm telescope at Observatoire de Haute Provence at the south of France, started in July 1994 and ended in July 2005 when the Sophie spectrometer replaced Elodie (Moultaka et al., 2004). We analyzed the spectra available when we began writing this paper in December 2006. Spectra of stars, galaxies, and other astronomical objects were taken regularly each night when the sky was clear enough, over a 10-year period, and more than 18 000 spectra are available on-line for intensive use of the Elodie archive (which contains 34 992 spectra). The on-line data reduction procedure removes scattered light and makes spectral wavelength and relative flux calibrations. Spectra are stored in Elodie archive in FITS (Flexible Image Transport System) format, a standard data format used in astronomy, endorsed by NASA and the International Astronomical Union (2007, http://fits.gsfc.nasa.gov/). Observations have been made by numerous astronomers, but most necessary information has been stored in the archive (like the time of the observation needed for astronomers for vari-

Table 1. Resolution, sampling, and spectral shift of H_2O at 592 nm.

Source	Sampling	HWHM	Shift
Reims, provided (cm^{-1})	list	0.096	−0.03
Reims, convolved (cm^{-1})	0.01	0.17	0
Elodie, theoretical (cm^{-1})	0.14	0.18	−4.93
Reims, convolved (nm)	0.00035	0.0065	0
Elodie, theoretical (nm)	0.005	0.0065	−0.163
This analysis (nm)	0.005	0.0090	−0.164
Equivalent $(m \times s^{-1})$	2532	3544	−83 050

Table 2. Results of spectral analysis on Elodie Archive, 18 318 spectra.

Value unit	Line-of-Sight amount 10^{22} molecule $\times cm^{-2}$	HWHM nm	Spectral Shift nm
Mean	6.00	0.00912	−0.163750
Minimum	0.00	0.00824	−0.16200
Maximum	20.00	0.01000	−0.16600
Step	0.02	0.00003	0.00002

able processes, the air-mass factor of the line-of-sight needed for information of the amplitude of atmospheric absorption lines, etc.). Unfortunately, some parameters such as atmospheric pressure around the observation site and humidity were not recorded or measured during observations. However, the astronomical data are so well referenced and the procedures identified so that the homogeneity of the data set is conserved. This paper is a demonstration of such homogeneity because no normalization factors have been applied from one result to another, or from one period to another. An example of a spectrum of the Elodie archive is presented in Fig. 2. The spectral range around 592 nm is displayed in Fig. 3. Not all astronomical spectra have as many visible absorption lines that are proper to solar type stars, here 51 Peg of spectral type G2. Some astronomical objects have only broad or a few lines visible, like hot O stars, or sometimes emission lines like nebulas. The wide range of sources make the spectral analysis more difficult, as we will discuss in the next section.

5   Spectral analysis

Our spectral analysis is composed of cyclic procedures, varying spectral resolution of water vapor cross-section, spectral shift of water vapor cross-section and n_{H_2O}, the total column of water vapor molecules per surface area in line-of-sight for each individual spectra. One cycle is calculated for one set

of these three parameters only. Note that there is no convergence procedure, and all possible cycles were evaluated in sequence. At the end of the analysis of each spectrum, the water vapor calculated is removed from the spectrum, i.e., its spectral signature substracted from the initial spectrum. The quality of the spectral analysis can be evaluated by the presence of water vapor signatures in the obtained spectrum: an efficient spectral analysis should remove any water vapor signature.

A spectral shift of $\Delta\lambda_{H_2O}$ is also applied to convert vacuum wavelength into air wavelength. The Shannon scheme (Shannon, 1949) is built for interpolation of cross-sections, and the water vapor optical thickness τ_{H_2O} measured with the Beer-Lambert law for the observation allows us to deduce water vapor line-of-sight amount of water vapor,

$$n_{H_2O} = \frac{\tau_{H_2O}}{\sigma_{H_2O}}. \tag{4}$$

The best values of n_{H_2O} are obtained by minimizing residuals, i.e. minimizing the standard deviation of $\ln(I_{0,\text{calculated}})$ after removing water vapor from spectra. A high quality residual reaches 0.005 while a low quality spectrum, or a spectrum with a dominant non-water vapor absorption or emission line in the spectral domain, increases residual up to 0.3. Values higher than 0.1, representing 0.1% of the data, are rejected in this analysis.

Figure 4 (dotted line) shows a water vapor cross-section calculated for spectrum of 51 Peg (Fig. 5) taken on November 1995. Applied spectral shift is not visible at this scale. The amount n_{H_2O} calculated is 7×10^{21} molecule$\times$cm^{-2}, giving an optical thickness represented by the upper dotted line on Fig. 5. The lower dotted line shows the spectrum before subtraction of water vapor signature, i.e., before analysis. The full line shows the spectrum after subtraction of water vapor signature, i.e., after analysis. Water vapor total column, N_{H_2O} is obtained by:

$$N_{H_2O} = \frac{n_{H_2O}}{\text{AMF}}. \tag{5}$$

AMF is the air-mass factor of the observation, i.e., the ratio between line-of-sight air column and vertical column above the observational point, a value provided in the Elodie archive and equivalent to $1 \div$ cosine of the source zenith angle for elevations larger than 20°. Note that for astronomers, objects are observed close to the meridian when possible, i.e. when the zenith angle is minimum. In present data set, less than 1.5% of observations are made at zenith angle higher than 70°.

6 Results and discussion

Results of the spectral analysis of all the spectra are summarized in Table 2, and values of N_{H_2O} are presented in Fig. 6. Mean value of the spectral shift measured during the analysis corresponds to the theoretical one presented in

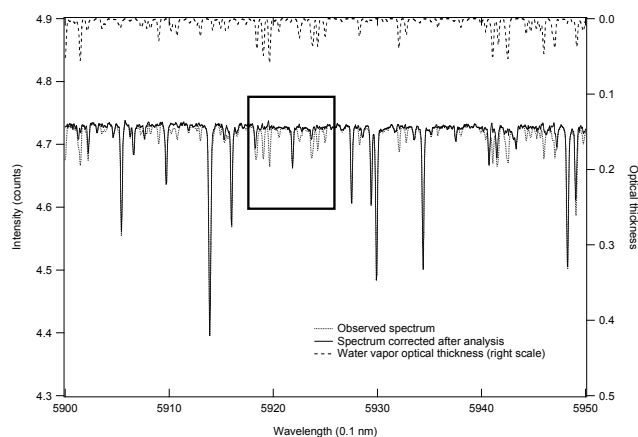**Fig. 5.** Optical thickness of H$_2$O in Elodie spectrum 199511010018 (right scale, dotted upper line). Respectively, dotted and full lines, spectrum and spectrum corrected from H$_2$O absorption.
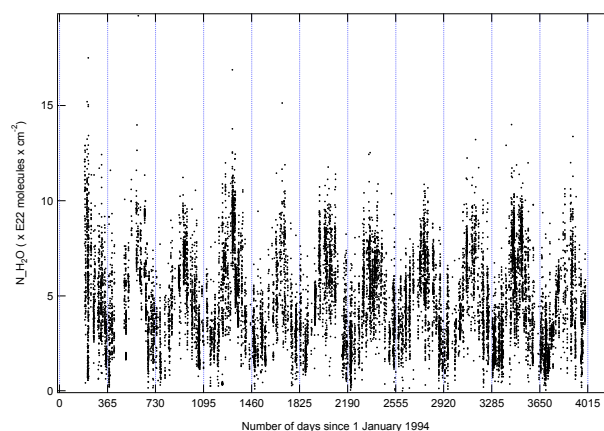

Fig. 6. Result of spectral analysis on 18 318 spectra of Elodie.

Table 1. Mean value of the HWHM measured during the analysis do not correspond to the theoretical one presented in Table 1 because atmospheric turbulences and effects on integration time and integration on the line-of-sight, i.e., with variable properties difficult to evaluate. The seasonal variation can be easily seen with higher values in summer and lower values in winter, an effect due to the variability of the dew point with atmospheric temperature. Sometimes, in winter, extremely low values are reached indicating the dryness of the atmosphere above Observatoire de Haute-Provence. For further interpretation, daily (nightly), weekly, and monthly means have been calculated from these results, as well as a simple sine curve fit (Fig. 7). A negative slope of $-0.44\pm0.24\times10^{22}$ molecule$\times$cm^{-2} per 10 years (i.e. -9.6% per decade) is obtained after removing the sine fit, indicating a not significant trend because it is not larger than two times its error. This is in agreement with the review of measured trends over Europe made by Morland et al. (2009). This negative slope might be introduced by the
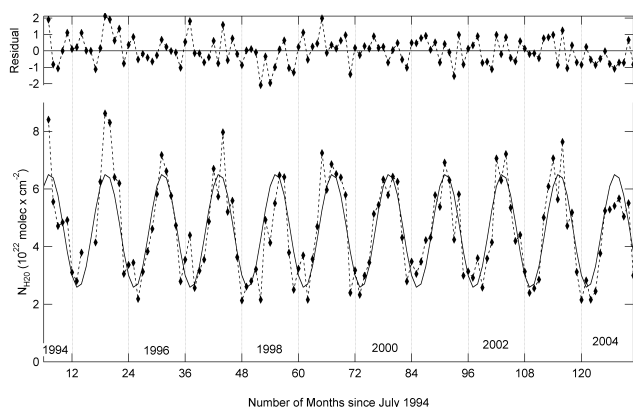
Fig. 7. H$_2$O monthly mean at OHP from 1994 to 2004 and a sine fit curve (dotted line) to show seasonal variation. The residual after subtraction of the sine fit, shown at the top of the graph, has a negative slope of $-0.44\pm0.24\times10^{22}$ molecule$\times$cm^{-2} per 10 years.

high summer values in 1994 and 1995. We believe that more detailed trend calculation, including seasonal trends calculations, could be made after we extend this analysis to the full Elodie Archive and to the Sophie Archive.

The first point for the discussion concerns the improvement of the building of water vapor cross-section, and its effect on error budget. Then, because most of the atmospheric parameters are not known, the retrieval process can be made using climatological atmospheric variability.

Secondly, saturation effects on strong absorption lines in the polyad 5ν range at 592 nm are not negligible and can reach up to 5% (Wagner et al., 2003). Such effects can be corrected by applying a linear correction factor depending on the quantity of water vapor, but we did not apply it at this stage. Our observations are made at low air-mass reducing enhancements of column amounts. Multiple scattering effects are reduced because astronomers make observations during clear skies. The spectral range chosen needs a lower correction factor than spectral ranges at higher wavelength. The very high spectral resolution of Elodie makes correction factor even lower than for low resolution instruments because individual lines are resolved. The amount of water vapor in the line-of-sight measured without correction is always lower than 30×10^{22} molecule$\times$cm^{-2}, and then saturation affects the linearity of Langley relation by less than 3% on less than 1% of all measurements, rending correction negligible when making monthly averages.

And thirdly, all observations are made at night during clear sky and it is possible that the water vapor trend estimation is biased.

In order to perform a validation of our measurements, they were used to calibrate lidar water vapor profiles obtained from May 1999 until December 2000 (Hoareau et al., 2009, as well as using radiosondes from Nîmes (the distance between OHP and Nîmes is less than 100 km). The calibration

procedure uses the variance between radiosonde profiles and lidar profiles between 2 and 8 km calibrated with our total column values on available days of lidar observation. This variance (0.4 at 2 km, nearly 1 at 5 km, decreasing to 0.6 g^2 kg^{-2} at 8 km) is due to the natural time variability of atmospheric water vapor at these altitudes. The decrease of this variance by few (5 to 10) percent observed when using Elodie water vapor data gives information on the sufficient validity of our measurements, but we need more co-located and simultaneous observations for better validation.

Our workflow is developed in the frame of the Astronomical Virtual Observatory and is available online as a web service, with results in VOtable format ready for interoperability (http://bdap.ipsl.fr/tellodie/, 2009). The concept of interoperability is already difficult to develop for astronomy and is even more complicated in interdisciplinary research, but this study is a demonstration that science-driven application can be developed more easily when using tools and standards of the Virtual Observatory.

7 Conclusions

We have presented water vapor total column measured at Observatoire de Haute-Provence between 1994 and 2004 using the Elodie archive: 18 318 spectra obtained by the Elodie high-resolution spectrometer on the 193-cm telescope. Seasonal variability of water vapor as well as a preliminary study of its trend above the observatory was possible because of the high quality of the available data. Astronomy can provide valuable past and present observations useful for atmospheric science, and this should be explored further. The large number of spectral databases in astronomy and their covering time periods, starting at the beginning of the previous century gives perspectives for extension of this workflow to ozone in the visible and for NO$_2$ at around 430 nm. The next step is to explore water vapor line shape sensitivity to air temperature and pressure and to extend this analysis to the full Elodie Archive and to the Sophie Archive.

Appendix A

Workflow in the Virtual Observatory

The Virtual Observatory is comprised of a workflow consisting of a group of tasks involving one or more sources, which may include data banks, web services, etc. The simplest workflow for an instrument in modern astrophysics is a series of tasks, usually called a pipeline. A pipeline has its own local and fixed input and output parameters, fixed by instrument conditions, and does not interfere with or depend upon external programs, parameters, or data. This is the main difference from the workflow. Pipelines are needed because data sources are permanently in evolution (new observations,
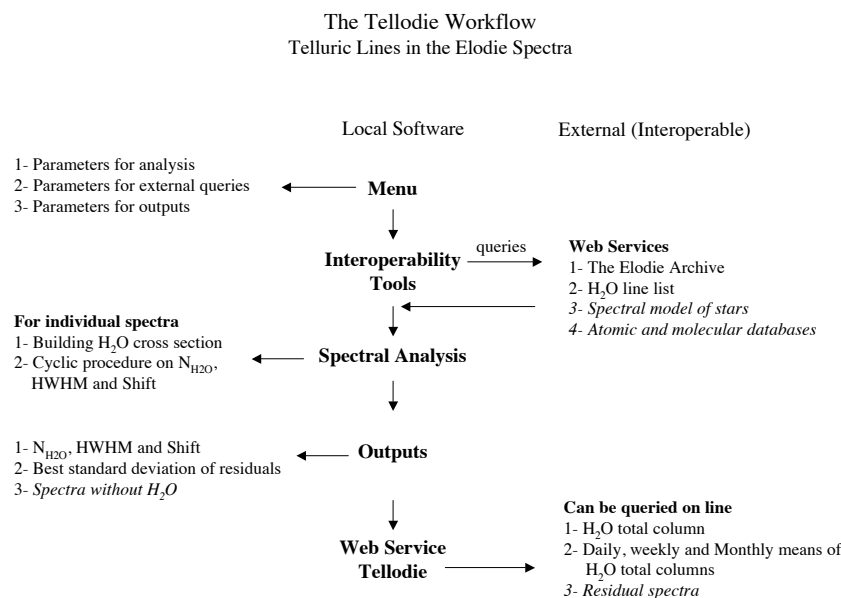
The Tellodie Workflow
Telluric Lines in the Elodie Spectra

Local Software   External (Interoperable)

1- Parameters for analysis
2- Parameters for external queries ← **Menu**
3- Parameters for outputs

↓

Interoperability   queries   **Web Services**
Tools   →   1- The Elodie Archive
                          2- H_2O line list
             ←   *3- Spectral model of stars*
                          4- Atomic and molecular databases

For individual spectra
1- Building H_2O cross section
2- Cyclic procedure on N_{H2O}, ← **Spectral Analysis**
   HWHM and Shift

↓

1- N_{H2O}, HWHM and Shift
2- Best standard deviation of residuals ← **Outputs**
3- *Spectra without H_2O*

↓

Web Service   **Can be queried on line**
Tellodie   →   1- H_2O total column
                     2- Daily, weekly and Monthly means of
                        H_2O total columns
                     3- Residual spectra

Fig. 8. Workflow diagram for derivation of water vapor from spectra. Options not used for this work are in italics.

improvement of a pipeline, update of available resources), whereas a workflow must integrate a complex approach of data treatment, including interactivity with other centers. Then, the interoperability between data centers, which is the basis of the Virtual Observatory, is the only way to make a reliable workflow. Not all the conditions of a workflow as defined by the Virtual Observatory, are present in our workflow, but we consider this a first step towards the minimum requirement.

The main goal of the workflow presented herein uses spectral analysis to retrieve amounts of trace gases. Although we focus on atmospheric water vapor, we can retrieve other gases such as NO_2 and ozone (Michalsky et al., 1995).

Our workflow is composed of four parts (Fig. 8): the menu, the search for sources (spectra, cross-sections, information on sources etc.), the spectral analysis, and the output. The menu is a user interface where one can select the type of workflow needed: some parameters like a selection of sources in time or high and low resolution analysis, and of course, the output format. Then, depending of selected parameters, the workflow searches for available components in an interoperable way. The search for sources is limited to the Elodie archive, but can easily be extended to other spectral archives. For example, a search for radial velocity variation studies is also plugged as an option, and this was the original objective during the initial development of this workflow. Today with limited options, our workflow will be extended and available as beta version to both astronomical and atmospheric communities. The main subject of this paper is the water vapor total column measurement whereas the spectral analysis contains several other outputs as well as a menu for input parameters. These are not presented in this study.

References

Angione, R. J.: Precipitable Water Vapor at Mount-Laguna Observatory, Publications of the Astronomical Society of the Pacific, 99(August), 895 pp., 1987.

Bastin, S., Champollion, C., Bock, O., Drobinski, P., and Masson, F.: On the Use of GPS Tomography to Investigate Water Vapor Variability During a Mistral/Sea Breeze Event in Southeastern France, Geophys. Res. Lett., 32, L05808, doi:10.1029/2004GL021907, 2005.

Challonge, D. and Divan, L.: Recherche sur les spectres continus stellaires, Ann. Astrophys., 15, 201–236, 1952.

Champollion, C., Masson, F., Van Baelen, J., Walpersdorf, A., Chery, J., and Doerflinger, E.: GPS monitoring of the tropospheric water vapor distribution and variation during the 9 September 2002 torrential precipitation episode in the Cevennes (southern France), J. Geophys. Res., 109, D24102, doi:10.1029/2004JD004897, 2004.

Coheur, P.-F., Fally, S., Carleer, M., Clerbaux, C., Colin, R., Jenouvrier, A., Mérienne, M.-F., Hermans, C., and Vandaele,

A. C.: New water vapor line parameters in the 26 000–13 000 cm^{-1} region, J. Quant. Spectrosc. Ra., 74, 493–510, 2002.

Coheur, P.-F., Clerbaux, C., Carleer, M., et al.: Retrieval of atmospheric water vapor columns from FT visible solar absorption spectra and evaluation of spectroscopic databases, J. Quant. Spectrosc. Ra., 82, 133–150, 2003.

Fally, S., Coheur, P.-F., Carleer, M., Clerbaux, C., Colin, R., Jenouvrier, A., Mérienne, M.-F., Hermans, C., and Vandaele, A. C.: Water vapor line broadening and shifting by air in the 26 000–13 000 cm^{-1} region, J. Quant. Spectrosc. Ra., 82, 119–131, 2003.

Fayt, C. and Van Roozendael, M.: WinDOAS 2.1 Software User Manual, BIRA-IASB, Brussels, Belgium, http://www.oma.be/BIRA-IASB/Molecules/BrO/WinDOAS-SUM-210b.pdf, 2001.

Fowle, F. E.: The Spectroscopic Determination of Aqueous Vapor, Astrophys. J., 35, 149–162, 1912.

Held, I. M. and Soden, B. J.: Water Vapor Feedback and Global Warming, Annu. Rev. Energ. Env., 25, 441–475, 2000.

Hoareau, C., Keckhut, P., Sarkissian, A., Baray, J.-L., and Durry, G.: Methodology for Water monitoring in Upper Troposphere with Raman Lidar at Observatory of Haute-Provence, J. Atmos. Ocean. Tech., in press, doi:10.1175/2009JTECHA1287.1, 2009.

Liu, X., Chance, K., Sioris, C. E., Newchurch, M. J., and Kurosu, T. P.: Tropospheric ozone profiles from a ground-based ultraviolet spectrometer: a new retrieval method, Appl. Optics., 45, 2352–2359, 2006.

Morland, J., Collaud Coen, M., Hocke, K., Jeannet, P., and Mätzler, C.: Tropospheric water vapour above Switzerland over the last 12 years, Atmos. Chem. Phys. Discuss., 9, 7239–7271, 2009, http://www.atmos-chem-phys-discuss.net/9/7239/2009/.

Michalsky, J., Liljegren, J., and Harrison, L.: A comparison of sun photometer derivations of total column water vapor and ozone to standard measures of same at the Southern Great Plains Atmospheric Radiation Measurement site, J. Geophys. Res., 100(D12), 25 995–26 003, 1995.

Moultaka, J., Ilovaisky, S. A., Prugniel, P., and Soubiran, C.: The ELODIE Archive, Publications of the Astronomical Society of the Pacific, 116, 693–698, 2004.

Perner, D. and Platt, U.: Detection of nitrous acid in the atmosphere by differential optical absorption, Geophys. Res. Lett., 6, 917–920, 1979.

Sarkissian, A.: Observation depuis le sol des nuages et poussières dans l'atmosphère: Applications à la stratosphère polaire et à l'atmosphère de Mars, Ph.D. thesis, 1992.

Sarkissian, A., Fish, D., Van Roozendael, M., Gil, M., Chen, H. B., Wang, P., Pommereau, J. P., and Lenoble, J.: Ozone and NO−2 air-mass factors for zenith-sky spectrometers: Intercomparison of calculations with different radiative transfer models, Geophys. Res. Lett., 22(9), 1113–1116, 1995.

Sarkissian, A.: Monitoring Stratospheric Constituents by Ground-based UV-visible Dobson and SAOZ spectrometers, European Research Courses on Atmosphere, edited by: Boutron, C., Volumn 4, Chapter X, 179–194, 2000.

Sarkissian, A.: Workflow for fast and simple analysis of Elodie spectra, invited paper at EPSC 1, Berlin, Germany, 18–22 September, 2006.

Sarkissian, A.: Détection de planètes extrasolaires par la méthode des vitesses radiales, in: Les Cahiers Clairaut, n 117, edited by: Paturel, G., Printemps, 2007.

Schneider, M., Hase, F., and Blumenstock, T.: Water vapour profiles by ground-based FTIR spectroscopy: study for an optimised retrieval and its validation, Atmos. Chem. Phys., 6, 811–830, 2006, http://www.atmos-chem-phys.net/6/811/2006/.

Shannon, C. E.: Communication in the presence of noise, Proc. Institute of Radio Engineers, 37(1), 10–21, 1949.

Tellodie: Telluric lines in the Elodie archive, Sarkissian, http://bdap.ipsl.fr/tellodie/, 2009.

Universite Libre de Belgique: Service de Chimie Quantique et Photophysique, http://www.ulb.ac.be/cpm/, 2007.

Vaughan, G., Roscoe, H. K., Bartlett, L., O'Connors, F. M., Sarkissian, A., Van Roozendael, M., Lambert, J.-C., Simon, P. C., Karlsen, K., Kastad Hoskar, B. A., Fish, D. J., Jones, R.L., Freshwater, R., Pommereau, J.-P., Goutail, F., Andersen, S. B., Drew, D. G., Hughes, P. A., Moore, D., Mellqvist, J., Hegels, E., Klupfel, T., Erle, F., Pfeilsticker, K., and Platt, U.: An intercomparison of ground-based UV-visible sensors of ozone and NO$_2$, J. Geophys. Res., 102, 1411–1422, 1997.

Wagner, T., Heland, J., Zöger, M., and Platt, U.: A fast H$_2$O total column density product from GOME -Validation with in-situ aircraft measurements, Atmos. Chem. Phys., 3, 651–663, 2003, http://www.atmos-chem-phys.net/3/651/2003/.

Westwater, E. R., Crewell, S., and Mätzler, C.: Surface-Based Microwave and Millimeter Wave Radiometric Remote Sensing of the Troposphere: a Tutorial, IEEE Geoscience and Remote Sensing Society Newsletter, 134, 16–33, 2005.